

Decay of spin-peierls state in $\text{CuGeO}_3\text{:Fe}$. The case of a strong disorder

S. V. Demishev*

*Low Temperatures Lab., General Physics Institute RAS, 38 Vavilov str., 117942, Moscow, Russia and
Venture Business Laboratory, Kobe University, 1-1 Rokkodai, Nada, Kobe 657-8501, Japan*

R.V.Bunting, A.A.Pronin, N.E.Sluchanko, and N.A.Samarin

Low Temperatures Lab., General Physics Institute RAS, 38 Vavilov str., 117942, Moscow, Russia

H.Ohta and S.Okubo

*Molecular Photoscience Research Center and Department of Physics,
Kobe University, 1-1 Rokkodai, Nada, Kobe 657-8501, Japan*

Y.Oshima

Graduate School of Science and technology, Kobe University, 1-1 Rokkodai, Nada, Kobe 657-8501, Japan

L.I.Leonyuk[†] and M.M.Markina

Moscow State University, 119899 Moscow, Russia

(Dated: Received November 7, 2018)

Influence of doping by iron impurity on spin-Peierls state in CuGeO_3 is studied. ESR measurements for the frequency/temperature domain 60-450 GHz/ 1.8-300 K and specific heat data obtained for the interval 6-20 K show that insertion of 1% of Fe completely destroy both spin-Peierls and antiferromagnetic orders. Damping of long-range magnetic order is accompanied by onset at $T < 20$ K of power asymptotics for magnetic susceptibility $\chi \propto T^{-\alpha}$ and magnetic part of specific heat $c_m \propto T^{1-\alpha}$, with the index $\alpha = 0.35-0.37$. This effect is characteristic to the limit of strong disorder for doped CuGeO_3 and may reflect formation of the Griffiths phase at low temperatures in $\text{CuGeO}_3\text{:Fe}$.

PACS numbers: 75.30Cr; 75.40.-s; 75.50.Lk

A. Introduction

$$c_m \propto T^{1-\alpha} \quad (2)$$

Discovery of inorganic spin-Peierls compound CuGeO_3 opened an opportunity to study influence of doping and disorder on the spin-Peierls state. Numerous experiments and theoretical studies have been carried out in this field up to now. However, from the theoretical point of view, most of the available data correspond to the limit of weak disorder when density of states have a pseudogap, i.e. a spin-Peierls gap filled by disorder-induced states [1]. In this case the expected temperature-concentration $T - x$ phase diagram consists of uniform state, spin-Peierls state, antiferromagnetic state and the region, where antiferromagnetic and spin-Peierls orders coexist [1]. This structure of $T - x$ phase diagram was observed experimentally for Zn, Si, Ni, Co, Mg and Mn impurities [1, 2, 3, 4, 5, 6, 7, 8, 9, 10].

In the limit of a strong disorder the ground state of CuGeO_3 is gapless and the density of states diverges at $\epsilon = 0$: $\rho(\epsilon) \propto |\epsilon|^{-\alpha}$ [1]. As a consequence the temperature dependences of magnetic susceptibility χ and magnetic contribution c_m to specific heat c_p acquire the forms [11]

$$\chi \propto T^{-\alpha} \quad (1)$$

where $\alpha < 1$. A non-Curie type behavior of $\chi(T)$ have been first reported for CuGeO_3 doped with Zn [4]. However, experiments in Ref.4 were carried out for extremely low Zn concentrations corresponding to the *weak* disorder limit, and the observed deviations from the Curie law can not be related to the case of strong disorder.

Recently Demishev et al. [12] suggested that CuGeO_3 doped with Fe provides a "true" experimental realisation of a strongly disordered regime [12]. It was found that substitution of Cu by 1% of Fe in CuGeO_3 matrix induces strong disorder in magnetic subsystem and leads to the complete damping of the spin-Peierls transition. As long as the low temperature asymptotic of the integrated intensity of the electron spin resonance (ESR) line $I(T)$ corresponded to Eq. (1), it was concluded that doping with iron gives rise to onset of a "quantum critical point" [12] or, in the other words, a strongly disordered limit [1, 11].

Nevertheless, the data presented in Ref.12 can not be considered as a complete evidence of the aforementioned conclusion. Firstly, the ESR frequency 60 GHz used in [12] was high enough to cause possible violation of the widely applied approximation $I(T) \propto \chi(T)$ [13]. Indeed, in general case the integrated intensity for arbitrary electromagnetic wave frequency ω and resonant magnetic field

[†]Deceased

*Electronic address: demis@lt.gpi.ru

B_{res} is given by [14]

$$I(T) \propto \omega \frac{M(T, B_{res})}{B_{res}} \quad (3)$$

and the observed in [12] deviations from Curie law may reflect non-linearity of magnetic moment $M(T, B_{res})$ in strong magnetic field (note that for $\omega/2\pi = 60$ GHz the resonant field in $\text{CuGeO}_3:\text{Fe}$ is about $B_{res} \approx 2$ T [12]).

Secondly, the iron concentration of 1% is relatively low and according to most findings should correspond to the weak disorder region [1, 2, 3, 4, 5, 6, 7, 8, 9, 10]. At the same time the absence of antiferromagnetic resonance (AFMR) modes in [12] was confirmed only up to $\omega/2\pi = 120$ GHz. Therefore the possibility of coexistence of ESR and AFMR, i.e. of spin-Peierls and antiferromagnetic orders, in high frequency range $\omega/2\pi > 120$ GHz for $\text{CuGeO}_3:\text{Fe}$ is not excluded. The described coexistence is a fingerprint of considerable but still weak disorder [1], so experiments at higher frequencies are highly desirable.

Thirdly, in the limit of a strong disorder Eqs. (1) and (2) should be valid simultaneously. This have not been checked in [12], moreover as far as we know the information about specific heat of the doped CuGeO_3 in this region is missing.

The aim of the present work is to solve experimentally these three problems formulated above and verify interpretation proposed in [12]. For that reason we studied single crystals of $\text{Cu}_{0.99}\text{Fe}_{0.01}\text{GeO}_3$ obtained by self-flux technique [15] and identical to the crystals studied in [12]. The quality of crystals have been controlled by X-ray and Raman scattering data; the actual contents of Fe in crystals was determined by chemical analysis. The structure of the samples studied coincided with the structure of pure CuGeO_3 and the effect of doping on the Raman spectra confirmed that iron impurity substitute cooper [12].

Experimental facilities of three different kinds were used to study magnetic and thermodynamic properties of $\text{CuGeO}_3:\text{Fe}$. Magnetoabsorption lines for the frequencies up to 450 GHz were studied with the help of the magneto-optical facility at Kobe University. In this experiment we measured transmission through the sample as a function of magnetic field B up to 16 T at fixed frequency for liquid helium temperatures 4.2 K and 1.8 K. Simultaneously a reference transmittance of the thin layer of DPPH powder has been recorded and both magnetoabsorption spectra of $\text{CuGeO}_3:\text{Fe}$ and DPPH were analyzed quantitatively.

Temperature dependence of the ESR spectrum in the range 1.8-140 K was measured using 60 GHz cavity spectrometer in General Physics Institute [12]. For each temperature studied the accuracy of the temperature stabilization was better than 0.01 K. All magnetoabsorption experiments reported below were carried out in $\mathbf{B} \parallel \mathbf{a}$ geometry.

Specific heat of $\text{CuGeO}_3:\text{Fe}$ for the temperature interval 6-20 K was studied in Moscow State University with

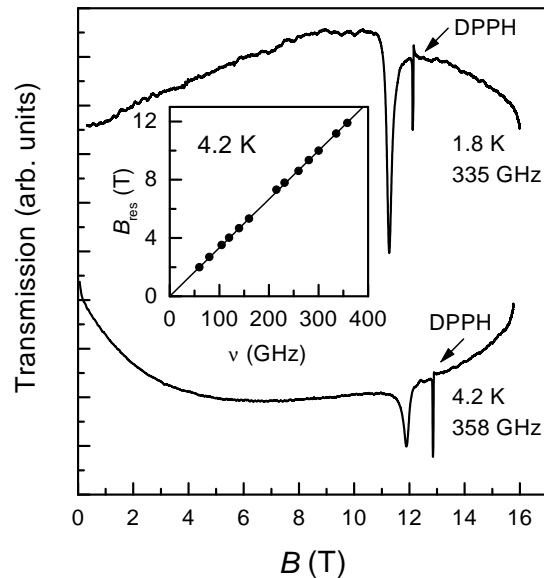


FIG. 1: Magnetoabsorption spectra for $\text{CuGeO}_3:\text{Fe}$ in transmission experiment.

the help of the low temperature small sample relaxation calorimeter.

B. ESR studies of $\text{CuGeO}_3:\text{Fe}$

Typical magnetoabsorption spectra in transmission experiment are shown in Fig. 1. Up to $\omega/2\pi = 450$ GHz neither additional "impurity" lines, nor AFMR modes have been detected and the spectrum for $\text{CuGeO}_3:\text{Fe}$ consists of a single lorentzian ESR line. The corresponding g -factor value is close to that for Cu^{2+} ions in the case $\mathbf{B} \parallel \mathbf{a}$ (see below). The resonant field for this line scales linearly with frequency, i.e. g -factor is frequency independent (see inset in Fig. 1).

Transmission data obtained at various frequencies were used to calculate ESR integrated intensities for $\text{CuGeO}_3:\text{Fe}$ and DPPH. It follows from Eq. (3) that for each frequency

$$\frac{I_1}{I_0} = \frac{M_1(T, B_{res}^1)}{M_0(T, B_{res}^0)} \cdot \frac{B_{res}^0}{B_{res}^1} \quad (4)$$

where indexes 0 and 1 denote characteristics of ESR lines for DPPH and $\text{CuGeO}_3:\text{Fe}$ respectively. Assuming that magnetic moment of DPPH is given by Brillouin function $M_0(T, B) \propto B_J(\mu_B B/k_B T)$ it is possible to calculate field or frequency dependence of magnetic moment $M_1(T, B_{res}) = f[B_{res}(\omega)]$ for $\text{CuGeO}_3:\text{Fe}$ with the help of Eq. (4). The result is presented in Fig. 2; it is visible that linear region $M_1 \propto B_{res}$ lasts up to $B_{res} \approx 6$ T ($\omega/2\pi = 200$ GHz). At higher resonant fields/frequencies magnetic moment of $\text{CuGeO}_3:\text{Fe}$ tends to saturate and

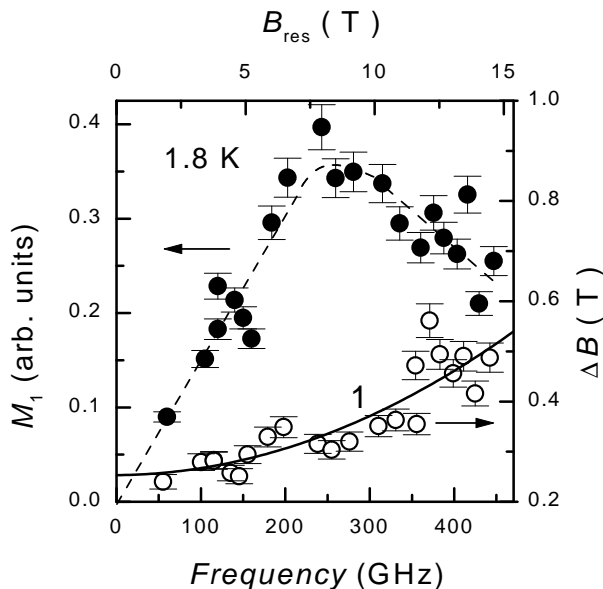


FIG. 2: Frequency and resonant field dependence of magnetic moment M_1 and ESR line width ΔB for $\text{CuGeO}_3:\text{Fe}$ at $T=1.8$ K. Curve 1 correspond to best fit of $\Delta B(\omega)$ using Eq. (5).

above $B_{res} \approx 11$ T ($\omega/2\pi = 350$ GHz) $M_1(B_{res})$ starts to decrease with field (Fig. 2).

Along with the integrated intensity the width ΔB of the ESR line in $\text{CuGeO}_3:\text{Fe}$ was calculated. Contrary to the frequency independent g -factor this parameter demonstrates a considerable frequency dependence. It follows from Fig. 2 that ΔB increases two times when frequency is varied from $\omega/2\pi = 60$ GHz to $\omega/2\pi = 450$ GHz. Experimental data $\Delta B(\omega)$ at $T=1.8$ K can be modeled by expression

$$\Delta B = A \cdot \omega^2 + C \quad (5)$$

which is characteristic to Raman relaxation mechanism for $S=1/2$ ion [16]. The line 1 in Fig.2 correspond to best fit parameters in Eq. (5) $A = (3.2 \pm 0.4) \cdot 10^{-7} \text{T/GHz}^2$ and $C = (0.063 \pm 0.004)$ T. It is interesting, that attempts to model $\Delta B(\omega)$ by expression for the direct process $\Delta B \propto \omega^5 / \tanh(\hbar\omega/2k_B T)$ [16] have failed as long as the theoretical frequency dependence was too strong to fit the experimental data in Fig. 2. Therefore it is possible to conclude that at low temperatures the dispersion of the relaxation time in $\text{CuGeO}_3:\text{Fe}$ is controlled mainly by the Raman process.

The above results indicate that at $\omega/2\pi = 60$ GHz the $\text{CuGeO}_3:\text{Fe}$ remains in the region of linear magnetic response and relation $I(T) \propto \chi(T) \equiv M(T, B_{res})/B_{res}$ is valid. In order to check assumptions of Ref. 12 we performed also temperature measurements of the ESR in the 60 GHz cavity spectrometer on the same crystal as

was investigated in the quasi-optical transmission experiment. For the precise determination of the g -factor a DPPH crystal was placed in the cavity together with the $\text{CuGeO}_3:\text{Fe}$ sample.

At all temperatures studied a single absorption line of lorentzian shape was observed (Fig.3), that is in agreement with the results of the quasi-optical experiment. Data in Fig.3 were used to calculate temperature dependences of the g -factor $g(T)$, line width $\Delta B(T)$ and integrated intensity $I(T)$ (see Fig.4).

For $T > 20$ K the value of the g -factor is $g \approx 2.15$ and characteristic to Cu ions in CuGeO_3 structure for geometry $\mathbf{B} \parallel \mathbf{a}$ [17]. Below $T = 20$ K g -factor starts to increase with lowering temperature and reach the value $g = 2.19$ at $T = 1.8$ K (Fig. 4). It is worth to note, that in the case of Fe-doped crystal no giant changes of the g -factor like in Ni-doped CuGeO_3 [8] are observed.

The temperature dependence of the line width is non-monotonic: when temperature is lowered the $\Delta B(T)$ first decreases, passes through a minimum at $T \approx 10-20$ K, and finally starts to increase again. It is interesting that in pure CuGeO_3 the width of the ESR line decreases gradually with lowering temperature and the magnitude of $\Delta B(T)$ at $T = 100$ K is about 6 times smaller than in Fe-doped crystal [17]. The decrease of temperature makes a difference in $\Delta B(T)$ more dramatic: at $T = 1.8$ K the line width for the Fe-doped CuGeO_3 is 200 times bigger than in pure crystal (see Fig. 4 and data from Ref.17).

The significant difference between pure and Fe-doped

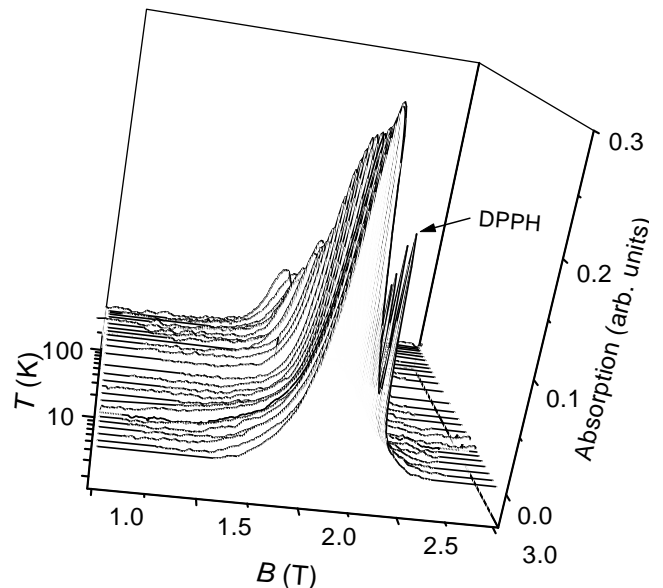


FIG. 3: Evolution of the ESR absorption line with temperature measured in cavity spectrometer ($\omega/2\pi = 60$ GHz, mode TE_{011} , quality factor $Q = 10^4$).

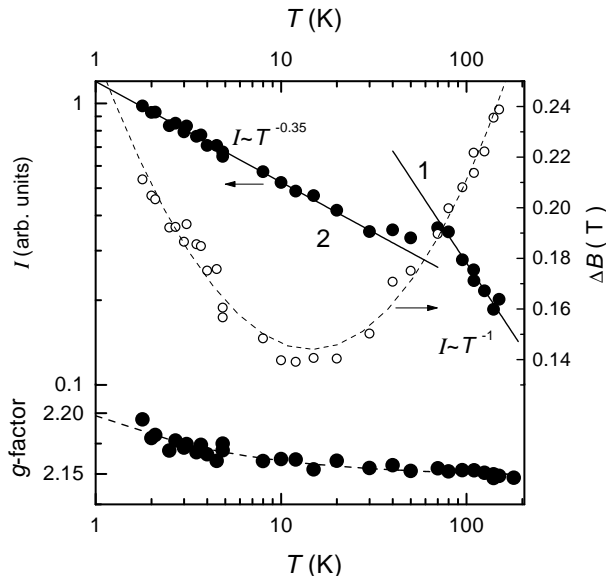


FIG. 4: Temperature dependences of the integrated intensity I , line width ΔB and g -factor obtained in cavity experiment.

CuGeO_3 is visible in the temperature dependence of the integrated intensity. It follows from Fig. 4 that in the Fe-doped crystal spin-Peierls transition is completely damped. For $T > 70$ K integrated intensity obeys Curie law $I(T) \propto T^{-1}$ (Fig. 4, curve 1). In the temperature range 25-70 K $I(T)$ saturates, and at lower temperatures a power law asymptotic behavior $I(T) \propto T^{-\alpha}$ with the index $\alpha = 0.35 \pm 0.03$ is observed (Fig. 4, curve 2). This result agrees well with the data obtained in Ref.12.

C. Specific heat in $\text{CuGeO}_3:\text{Fe}$

The experimental limitation on the sample mass in specific heat measurements has not allowed to study individual crystals as in ESR experiments and a set of $\text{CuGeO}_3:\text{Fe}$ single crystals cleaved from the same ingot and having total mass about 40 mg have been used. The temperature dependence of specific heat $c_p(T)$ for Fe-doped and pure CuGeO_3 is presented in Fig. 5 (curves 1 and 4 respectively). The sharp peak at spin-Peierls transition in $\text{CuGeO}_3:\text{Fe}$ sample have vanished, that is in agreement with the ESR evidence of complete damping of the spin-Peierls transition by iron impurity (Fig. 4).

From the fact that in Fe-doped crystal specific heat is considerably (about 50% for $T > 14$ K) bigger than in pure CuGeO_3 (Fig. 5) it is reasonable to suppose that the studied sample has an excessive magnetic contribution $c_m(T)$ in $c_p(T)$:

$$c_p(T) = c_D(T) + c_m(T) = \beta T^3 + \gamma T^\delta \quad (6)$$

Here the first term represents lattice (Debye) part and the choice for the analytical representation of the magnetic term $c_m(T) = \gamma T^\delta$ is made in accordance with Eq. (2).

The Eq. (6) was applied to model experimental data for $\text{CuGeO}_3:\text{Fe}$ (Fig. 5). We find the value $\beta = (0.36 \pm 0.02)$ mJ·mol/K, corresponding to Debye temperature $\Theta_D \approx 300$ K. This result agrees well with the previous findings for pure CuGeO_3 [18], where $\Theta_D = 310$ K have been obtained. Consequently the main changes in specific heat caused by doping with iron occur in magnetic part $c_m(T)$ (see curve 2 in Fig. 5; the magnetic contribution is obtained by subtracting of the lattice part from $c_p(T)$). The best fit of $c_m(T)$ gives parameters values $\delta = 0.63 \pm 0.04$ and $\gamma = (0.44 \pm 0.04)$ mJ·mol/K $^{1+\delta}$. The power law for magnetic part of specific heat is illustrated by inset in Fig. 5.

D. Summary and discussion

Summarizing experimental results of the present work, we wish to mark that observed low temperature behavior of the ESR line reflects intrinsic properties of Cu^{2+} chains modified by Fe impurity rather than impurity paramagnetism caused by Fe ions. This conclusion can be deduced from the g -factor values characteristic to Cu^{2+} (Fig. 4) and the observation of the line width frequency dependence given by Eq. (5). Indeed, for the Fe^{2+} ion substituting Cu^{2+} ion in $S = 1/2$ chain a spin state with $S = 2$ may be expected [19]. For the integer impurity spin the

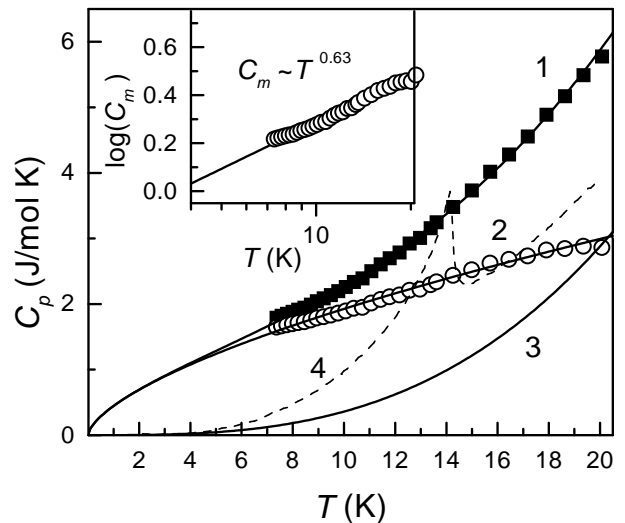


FIG. 5: Temperature dependence of specific heat in $\text{CuGeO}_3:\text{Fe}$. Curve 1: points- experiment, line- best fit using Eq. (6). Curve 2: points- experimental data for magnetic specific heat obtained from $c_p(T)$ by subtraction of the lattice contribution (curve 3); line- best fit of magnetic part. Curve 4- specific heat for pure CuGeO_3 (from [18]).

term proportional to ω^2 in expression for the line width should vanish and $\Delta B(T)$ will be frequency independent [16]. The expected "impurity behavior" for Fe^{2+} contradicts to experimental data (Fig. 2) and the whole experimental picture of ESR in $\text{CuGeO}_3\text{:Fe}$ is consistent with the assumption that magnetic properties of this system are controlled by disordered Cu^{2+} chains. The presence of the disorder in magnetic subsystem follows from the strong broadening of the ESR line with respect to the pure crystal (Fig. 4 and Ref.17) and agrees with the results of the structural studies [12].

As long as the integrated intensity measured at $\omega/2\pi = 60$ GHz for $\text{CuGeO}_3\text{:Fe}$ is proportional to magnetic susceptibility, the latter quantity diverges at $T < 20$ K: $\chi(T) \propto T^{-\alpha}$, where $\alpha \approx 0.35$. According to Eq. (2) the value of the index δ in Eq(6) should be $\delta = 1 - \alpha \approx 0.65$, whereas experiment gives $\delta = 0.63$ (Fig. 5). Both values of the indexes are coincide within the experimental error and therefore Eq. (1) and Eq. (2) are hold simultaneously. This result confirms that inserting of 1% of iron in CuGeO_3 matrix really induces a strongly disordered limit of doping as it was proposed in [12].

From the theoretical point of view the non-Curie asymptotic behavior of magnetic susceptibility and related power law for magnetic part of specific heat reflect the onset of the Griffiths phase (GP) which thermodynamic properties are controlled by relatively rare spin clusters correlated more strongly than average [20-22]. The GP appears in various spin systems below some critical temperature T_G if the magnitude of random potential is strong enough to destroy transition to magnetically or-

dered phase [20-22] (in the case of $\text{CuGeO}_3\text{:Fe}$ we have shown that both spin-Peierls and antiferromagnetic transitions are completely damped by doping). According to the data in Fig. 4 the value of T_G in $\text{CuGeO}_3\text{:Fe}$ can be estimated as $T_G = 20-40$ K. The possible interaction effects inside spin clusters of GP may be also responsible for a weak temperature dependence of the g -factor observed at $T < T_G$ (Fig. 4) and unusual field dependence of magnetic moment (Fig. 2). However this problem requires further theoretical investigation.

It is interesting, that 1% of iron is sufficient to shift doped CuGeO_3 into the region of the strong disorder, whereas another impurities studied [1, 2, 3, 4, 5, 6, 7, 8, 9, 10] have corresponded to a weak disorder limit [1]. This question deserves a detail discussion of the universal properties of $T - x$ phase diagram of CuGeO_3 and is reserved for future publications.

Acknowledgments

Authors are grateful to A.N.Vasil'ev for valuable discussions and V.V.Glushkov for assistance. This work was supported by programmes "Physics of Microwaves" and "Fundamental Spectroscopy" of Russian Ministry of Industry, Science and Technology. SVD acknowledge financial support from Venture Business Laboratory in Kobe University.

-
- [1] M.Mostovoy, D.Khomskii, and J.Knoester, Phys. Rev. B **58**, 8190 (1998)
- [2] Y.Sasago, N.Koide, K.Uchinokura et al., Phys. Rev. B **54**, R6835 (1996)
- [3] S.Koad, J.-G.Lussier, D.F.McMorrow, and D.McK Paul, J.Phys.: Condens. Matter **8**, 6251 (1996)
- [4] K.Manabe, H.Ishimoto, N.Koide et al., Phys. Rev. B **58**, R575 (1998)
- [5] H.Nojiri, T.Hamamoto, Z.J.Wang et al., J.Phys.: Condens. Matter **9**, 1331 (1997)
- [6] B.Grenier, J.-P.Renard, P.Veillet et al., Phys. Rev. B **57**, 3444 (1998)
- [7] P.E.Anderson, J.Z.Liu, and R.N.Shelton, Phys.Rev. B **57**, 11492 (1998)
- [8] V.N.Glazkov, A.I.Smirnov, O.A.Petrenko et al., J.Phys.: Condens. Matter **10**, 7879 (1998)
- [9] T.Masuda, A.Fujioka, Y.Uchiyama et al., Phys. Rev. Lett. **80**, 4566 (1998)
- [10] P.E.Anderson, J.Z.Liu, and R.N.Shelton, Phys. Rev. B **56**, 11014 (1997)
- [11] L.N.Bulaevskii, A.V.Zvarykina, Yu.S.Karimov et al., Sov. Phys. JETP **35**, 384 (1972)
- [12] S.V.Demishev, R.V.Bunting, L.I.Leonyuk et al, JETP Letters **73**, 31 (2001)
- [13] S.A.Al'tshuler and B.M.Kozyrev, Electron Paramagnetic Resonance (Academic Press, New York and London, 1964), p.15
- [14] C.Kittel, Introduction to Solid State Physics (Fourth edition, J.Wiley Sons, New York, London, Sydney, Toronto), ch. 17
- [15] S.V.Demishev, L.Weckhuysen, J.Vanacken et al., Phys. Rev. B **58**, 6321 (1998)
- [16] A.Abragam and B.Bleaney, Electron Paramagnetic Resonance of Transition Ions (Clarendon Press, Oxford, 1970)
- [17] S.V.Demishev, A.V.Semenov, N.E.Sluchanko et al., JETP **85**, 943 (1997); H.Ohta, S.Imagawa, H.Ushiroyama et al., J. Phys. Soc. Jpn. **63**, 2870 (1994); Y.Yamamoto, H.Ohta, M.Motokawa et al., J. Phys. Soc. Jpn. **66**, 1115 (1997)
- [18] X.Liu, J.Wosnitza, H.v.Lohneysen, and R.K.Kremer, Phys. Rev. Lett. **75**, 771 (1995)
- [19] W.Low, Paramagnetic Resonance in Solids (Academic Press, New York and London, 1960)
- [20] R.B.Griffiths, Phys. Rev. Lett. **23**, 17 (1969)
- [21] D.S.Fisher, Phys. Rev. Lett. **69**, 534 (1992); Phys. Rev. B **50**, 3799 (1994); Phys. Rev. B **51**, 6411 (1995)
- [22] A.Rosch, in Abstracts of LT22, Helsinki, 1999, p.389